Ribavirin induces widespread accumulation of IMP dehydrogenase into rods/rings structures in multiple major mouse organs

Gerson Dierley Keppeke[a,*], S. John Calise[b], Edward K.L. Chan[b], Luis Eduardo C. Andrade[a]

[a] Rheumatology Division, Escola Paulista de Medicina, Universidade Federal de São Paulo, Rua Botucatu 740, São Paulo, SP, 04023-062, Brazil
[b] Department of Oral Biology, University of Florida, 1395 Center Drive, Gainesville, FL, 32610-0424, USA

A B S T R A C T

Ribavirin (RBV) is a guanosine analogue triazole most commonly used in the treatment of chronic hepatitis C (HCV) infection. Although its mechanism of action is a matter of debate, several possibilities have been proposed, including depletion of guanine nucleotides through inhibition of inosine monophosphate dehydrogenase (IMPDH). IMPDH has been shown to assemble into micron-scale rod- and ring-shaped structures (rods/rings or RR), also called "IMPDH filaments," both *in vitro* and *in vivo*. Formation of RR structures can occur naturally, potentially to influence IMPDH activity, or when *de novo* guanosine monophosphate biosynthesis or IMPDH itself are inhibited by nutrient deprivation or drugs like RBV. Numerous studies have also reported the occurrence of autoantibodies targeting RR structures (anti-RR) in HCV patients previously treated or under treatment with interferon-α and ribavirin (IFN/RBV) combination therapy. For this brief study, we considered the strong association between RR autoantibodies and IFN/RBV treatment, and the lack of data assessing how RBV affects RR formation in a variety of tissues *in vivo*. First, RR structures formed in the spleen and pancreas of normal mice without any treatment. Then, in RBV-treated mice, we detected RR structures in a number of tissues, including stomach, liver, spleen, kidney, brain, skin, and cardiac and skeletal muscle. We made several intriguing observations: predominance of RR structures in the mucosa and submucosa layers of the stomach wall; a high proportion of RR-positive cells in the cerebral cortex, suggesting that RBV actually crosses the blood-brain barrier; and a higher ratio of rings to rods in the epidermis compared to the dermis layer of the skin. Screening for RR structures appears to be a useful method to track tissue penetration of RBV and the many RR-inducing drugs previously identified.

1. Introduction

In recent years, numerous studies have reported the occurrence of autoantibodies targeting micron-scale rod- and ring-shaped structures (rods/rings or RR, also called cytoophidia) in the cytoplasm of cells (Calise et al., 2014; Carcamo et al., 2011, 2014). The primary autoantigen of these rods/rings autoantibodies (anti-RR), and major component of RR structures, is the enzyme inosine monophosphate dehydrogenase (IMPDH) (Calise et al., 2018; Carcamo et al., 2011; Keppeke et al., 2015; Probst et al., 2013; Seelig et al., 2011). IMPDH catalyzes the rate-limiting step in *de novo* guanosine monophosphate (GMP) synthesis and is an important target for immunosuppressive and antiviral drugs. Some of these IMPDH inhibitors, such as azathioprine, mycophenolic acid, mizoribine, and ribavirin (RBV), are currently used by an array of patients around the world. In cultured cells, IMPDH inhibitors promote the rapid polymerization of IMPDH protein into RR structures (Carcamo et al., 2011; Gunter et al., 2008; Ji et al., 2006). Other drugs that target upstream or downstream of IMPDH to block GMP synthesis, such as acyclovir, methotrexate, and pemetrexed, cause similar RR formation (Calise et al., 2016b; Carcamo et al., 2014; Keppeke et al., 2016b). RR formation has also been demonstrated in the peripheral blood mononuclear cells (PBMCs) of patients taking azathioprine, mycophenolic acid, methotrexate, and RBV (Keppeke et al., 2016b). Based on the potency of these drugs, it is reasonable to investigate the extent of RR formation across tissues of living organisms.

Despite the potential for a variety of drugs to cause RR formation in humans, RR autoantibodies are almost exclusively found in patients with chronic hepatitis C virus (HCV) infection that have been exposed

to interferon-α and ribavirin (IFN/RBV) combination therapy (Calise et al., 2016a; Covini et al., 2012; Keppeke et al., 2012; Novembrino et al., 2014; Stinton et al., 2013). Remarkably, RR autoantibodies are not found in these same patients prior to treatment, and are detected only very rarely in other diseases or in healthy individuals (Calise et al., 2014; Climent et al., 2016). Thus, we have referred to the production of RR autoantibody as a human model of drug-induced autoantibody generation, considering that the particular combination of IFN/RBV exposure and presence of HCV appears to enhance the immunogenicity of IMPDH. The drug-induced RR autoantibody production is extensively discussed elsewhere (Calise et al., 2015; Keppeke et al., 2016a).

Even 40 years after the discovery of its broad antiviral activity, the mechanism of action of RBV in HCV treatment remains a matter of debate (Paeshuyse et al., 2011). Several modes of action have been proposed, such as the depletion of guanine nucleotides through inhibition of IMPDH, direct inhibition of viral RNA-dependent RNA polymerases, modulation of cellular and humoral immunity, or even the increased mutagenesis of HCV leading to non-infectious virions (Galli et al., 2018; Testoni et al., 2014). Although recently developed direct-acting antivirals (DAAs) have promised better interferon-free sustained virological response for HCV patients, RBV seems to be important for many DAAs to exert their full clinical benefits (Welsch et al., 2012). RBV is a triazole analogue of guanosine, and its distribution in tissues is largely defined by the expression of nucleoside transporters shown to facilitate the uptake of RBV (Endres et al., 2009). However, improved understanding of the penetration of RBV into different tissues *in vivo* could be useful in elucidating its antiviral effects, especially since we do not know why RR autoantibodies are preferentially observed in IFN/RBV-treated patients and seldom in patients receiving other RR-inducing drugs.

For this brief study, we considered the strong association between RR autoantibodies and IFN/RBV treatment, and the lack of data assessing how RBV affects RR formation in a variety of tissues *in vivo*. To understand this, we treated mice with RBV, collected various tissues, and probed them with rabbit polyclonal anti-IMPDH and human anti-RR positive serum. Strikingly, we detected RR structures in all tissues collected from RBV-treated mice, including stomach, liver, spleen, kidney, brain, skin, and cardiac and skeletal muscle tissues. In contrast, the distribution of RR structures in control untreated mice was restricted to the spleen and pancreas.

2. Results/discussion

As a control for the experimental group, tissues from untreated mice were collected and probed with anti-IMPDH alone or double-stained with anti-IMPDH and anti-RR serum as described in Supplementary Table 1. No RR structures were detected in stomach, liver, kidney, brain, skin, or cardiac and skeletal muscle tissues (Fig. 1A and B and Supplementary Fig. 1). These data indicate that the widespread occurrence of RR structures in the tissues of RBV-treated mice was a result of the drug intake (Fig. 2).

Surprisingly, we detected RR structures in 16% of cells in spleen sections from the untreated mice. Curiously, the structures appeared predominantly in the outer edges of the spleen near the capsule, but only in the red pulp (Fig. 1C, D, F). Since RR structures were not present in all cells in the red pulp, and several different types of blood cells can be found in this region, further studies must be done to identify exactly which cell types form the RR structures.

A prior study demonstrated the presence of IMPDH-based RR structures in mouse pancreatic islet cells (Chang et al., 2015). The authors proposed that RR structure formation correlates with insulin secretion in pancreatic β cells, since insulin-exocytosis-associated GTPases utilize GTP to promote insulin secretion. Although we did not analyze the pancreas in the RBV-treated mice, we did stain for IMPDH in untreated mouse pancreas, and found RR structures in 15% of cells (Fig. 1E and F). This reinforces the idea that RR structure formation

may be a common occurrence in specific tissues *in vivo*, and thus RR structures are likely to be performing important physiological functions.

We previously demonstrated that RR structures form in the PBMCs of HCV patients several months into RBV therapy (Keppeke et al., 2016b). To determine whether *in vivo* RR formation after RBV treatment is a widespread occurrence, rather than restricted to white blood cells, we treated mice with RBV, collected various tissues, and probed them with rabbit anti-IMPDH and human anti-RR serum (Supplementary Table 1). Strikingly, we detected RR structures in all tissues collected from RBV-treated mice.

In the stomach wall, although the overall proportion of cells with RR structures was high (58%), RR structures formed predominantly in the mucosa and submucosa layers (Fig. 2A, representative images and Fig. 2I, quantification of all tissues). This might be because these cells came into direct contact with the orally ingested RBV, which can rapidly cross the plasma membrane with the help of nucleoside transporters. Additionally, the muscularis layer of the stomach is smooth muscle, and the other muscle tissues we examined also showed a lower proportion of RR-positive cells (Fig. 2I). It is worth mentioning that the RR structures were recognized by both anti-IMPDH and anti-RR serum with perfect colocalization, as exemplified in Fig. 2A′, reinforcing the IMPDH-based composition of RR and the previous observation that this anti-RR positive serum contains autoantibodies to IMPDH (Carcamo et al., 2011).

The organ with the highest overall proportion of RR-positive cells was the liver (71%) (Fig. 2B, I). Recent evidence shows that RBV efficiently loads into the liver, with total hepatic metabolite concentrations exceeding maximal levels in plasma by approximately 30-fold (Babusis et al., 2018). This indicates that hepatocytes may trap phosphorylated RBV metabolites. We expected that RBV would have high penetration in the liver, considering its use in the treatment of chronic HCV, which primarily infects the liver. Additionally, *in vitro* tests showed that the proportion of RR-positive cells reflects the concentration of RR-inducing drugs, up to a certain level (Keppeke et al., 2016b).

The proportion of RR-positive cells was relatively low in the spleen (21%) and moderate in the kidney (39% of cells) (Fig. 2C, D, I). The renal excretion of RBV and its metabolites accounts for 40% of its clearance; the remainder is eliminated through the spleen via its principal metabolite, RBV triphosphate, which is captured in erythrocytes (Carrier et al., 2016). After ingestion, once inside the cells, RBV is phosphorylated by adenosine kinase into its active monophosphate, diphosphate, and triphosphate forms (Markland et al., 2000). RBV monophosphate binds and inhibits IMPDH, but it is not known if other phosphorylated forms of RBV contribute to RR formation (Gish, 2006). Intriguingly, we did not observe any difference between RR formation in the spleens of untreated (16% ± 3.8% of cells) and RBV-treated mice (21% ± 4.9%; p = 0.45, Student's t-test), and in both cases RR predominated in the red pulp. It might be that RBV monophosphate, which inhibits IMPDH and is presumably the major form of RBV that induces RR formation, does not reach significant levels in the spleen compared to RBV triphosphate.

Cardiac and skeletal muscle sections also showed low overall proportions of RR-positive cells, 13% and 24%, respectively (Fig. 2E, F, I). We recently demonstrated a positive correlation between the presence of RR structures and high cell proliferation rate, associated with increased demand for guanine nucleotides in cells (Keppeke et al., 2018). Cardiomyocytes and myofibers, the most common cells in cardiac and skeletal muscle, respectively, do not proliferate in mature muscle tissues. Consequently, demand for *de novo* guanine nucleotide biosynthesis is also likely to be low, as fiber cells prefer ATP instead of GTP as an energy source. This might explain why the observed proportions of RR structures were decreased in these tissues. However, it is interesting that RBV induced RR structure formation even in non-dividing muscle cells.

The observed proportion of RR-positive cells in the cerebral cortex
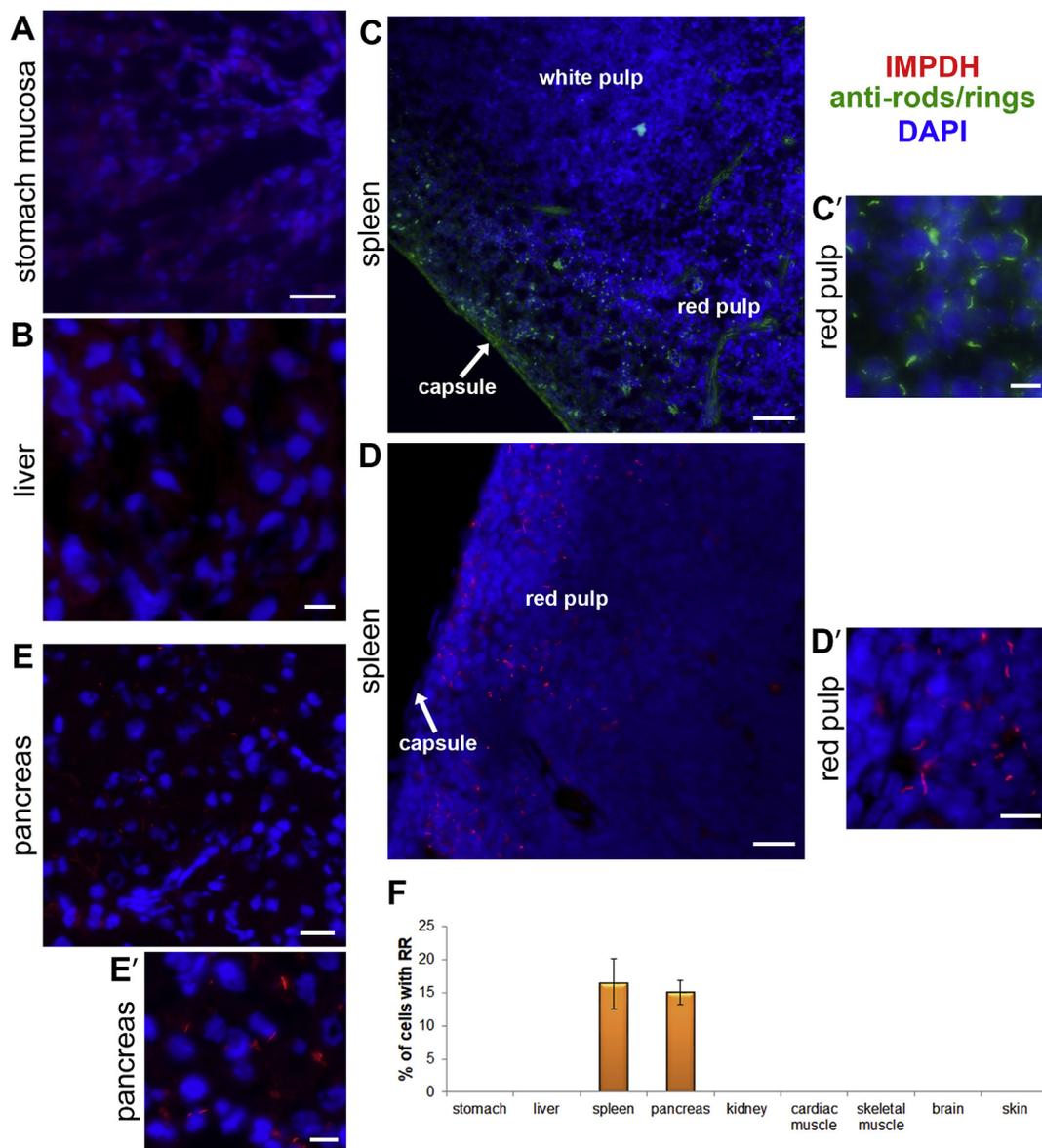
Fig. 1. RR structures formed in the spleen and pancreas of untreated mice. Cryosections from untreated mice (n = 3) were labeled with anti-IMPDH (red) or human anti-RR serum (green). **(A, B)** Stomach mucosa and liver sections showed no RR structures. **(C, D)** Spleen sections from untreated mice showed RR structures labeled by anti-RR serum (C) and by anti-IMPDH antibody (D). RR structures primarily formed in the outer edges of the spleen, in the red pulp near the capsule. **(E)** RR structures were also detected in pancreas sections. Scale bars: 50 μm in A, C, and D; 30 μm in E; 10 μm in B, C′, D′, and E′. **(F)** Overall percentage of cells that formed RR structures in the different tissues analyzed. Error bars indicate SEM. Additionally to stomach and liver (A, B), representative images for the other tissues analyzed that did not show any RR structures are presented in Supplementary Fig. 1.

was 56% (Fig. 2G, I). RBV has been shown to be ineffective against several encephalitis viruses in mice after intraperitoneal, subcutaneous, or intramuscular injection (Bussereau et al., 1988; Sidwell et al., 1973), suggesting a failure of RBV to effectively cross the blood-brain barrier. Attempts have been made to conjugate RBV to cyclodextrin as a drug carrier, or find new administration routes, such as intranasal, to overcome this issue (Colombo et al., 2011; Jeulin et al., 2009). The presence of RR structures in brain cells suggests that RBV actually crosses the blood-brain barrier, although we do not know if the amount entering the brain is sufficient for antiviral action. The presence of RR structures could be an effective criterion to determine if RBV or other RR-inducing drugs (Keppeke et al., 2016b) cross the blood-brain barrier.

In most tissues and cell lines, rods predominate over rings. In the skin, the overall percentage of RR-positive cells was 37%, but, unexpectedly, the proportion of rings (rather than rods) was higher in the epidermis (58% ± 6.3%) than dermis (17% ± 5.9%; p = 0.002 by Student's t-test) (Fig. 2H and I). A higher proportion of rings was previously observed in mouse embryonic stem cells (~90%) in contrast to cancer cell lines (~20%) (Carcamo et al., 2011). Recently, we showed additional evidence that rods and rings are likely functionally equivalent, since rods can become rings, merge with rings, or the structure can initially form as a ring (Chang et al., 2018). The reason for and meaning of the predominance of rings over rods in a restricted set of tissues is currently unknown. Further examination of skin tissue in RBV-treated mice could improve our understanding of the conditions in which cells prefer to assemble either the rod or the ring form of the RR structures.

3. Conclusion

Our main goal in this study was to evaluate if IMPDH-based RR formation occurs in other tissues and cell types beyond PBMCs, reported earlier in patients undergoing IFN/RBV therapy. We detected
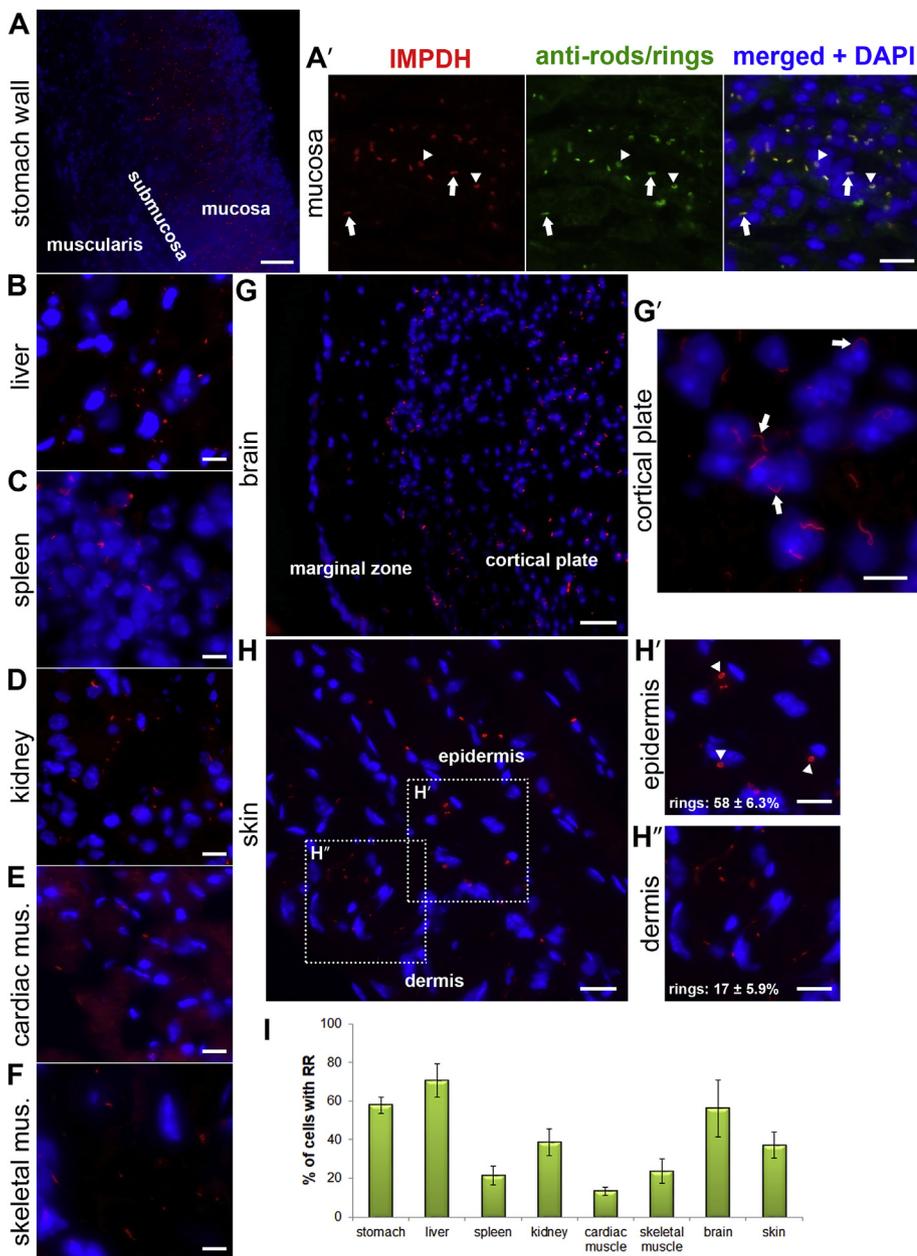
Fig. 2. RBV induced assembly of RR structures in a variety of mouse tissues. Mice (n = 3) were treated for three months with RBV before tissues were harvested and snap-frozen. Cryosections were labeled with anti-IMPDH (red) or human anti-RR serum (green). **(A)** Stomach wall sections showed numerous RR structures, primarily in the mucosa and submucosa layers. **(B–F)** RR structures were observed in sections of various organs (liver, spleen, and kidney) and muscle (cardiac and skeletal). **(G)** Brain sections showed RR formation predominantly in the cortical plate. **(H)** RR structure formation in skin sections. The epidermis layer showed a higher proportion of rings (58% ± 6.3%) than dermis (17% ± 5.9%; p = 0.0021 by Student's t-test). Arrows indicate rods and arrowheads indicate rings in (A′), (G′) and (H′). Scale bars: 50 μm in A; 30 μm in G and H; 10 μm in A′, B-F, G′, H′, and H″. **(I)** Overall percentage of cells with RR structures in the different tissues analyzed. Error bars indicate SEM. Liver, stomach, and brain were the tissues with the highest proportions (> 50%) of cells forming RR structures.

widespread *in vivo* assembly of RR structures in all tissues analyzed from RBV-treated mice. We made several original and intriguing observations: RR structures predominated in the mucosa and submucosa layers of the stomach; there was a high proportion of RR-positive cells in the cerebral cortex; and there was a higher proportion of rings over rods in the epidermis compared to the dermis in the skin. Additionally, we detected RR structures in restricted tissues of normal mice without any treatment. Adding to a previous report on the presence of RR-positive pancreatic cells in untreated mice, we also discovered RR structures in the spleen, although we could not identify the specific cell type that formed RR structures in the red pulp. These data suggest that RR formation is a physiological process and may play an important role in the purine biosynthesis pathway under specific circumstances.

In recent years, we and others have independently reported that a high percentage of chronic HCV patients treated with IFN/RBV produce autoantibodies against IMPDH or other undetermined components of RR structures, yielding a positive HEp-2 immunofluorescence test for the RR pattern (Calise et al., 2015; Keppeke et al., 2016a). Although we do not fully understand the clinical implications of producing RR

autoantibodies and the widespread formation of RR structures after RBV intake, we would recommend caution be exercised in the use of this drug to avoid overdosage and unnecessary prolonged exposure. As shown in this study, RBV can induce RR structure formation in a variety of organs, not just the liver, with unknown consequences. We also want to point out that screening for RR structures could be a useful method to track tissue penetration of the many RR-inducing drugs we have previously identified (Keppeke et al., 2016b).

4. Methods

Six male, 8-week-old BALB/c mice were obtained for the study. Three were kept untreated as controls, while the other three were treated orally with ribavirin for three months (generic ribavirin, lot # 14030216, Farmanguinhos Laboratory/Fiocruz, Rio de Janeiro, Brazil). Ribavirin was diluted in the water supplied to the mice, which was replaced every three days. Considering the daily intake of water per mouse, ribavirin intake was equivalent to 0.4 mg/day, a bodyweight-based dose similar to the daily concentration used in the treatment of

chronic HCV infection in humans. The mice were maintained at CEDEME, an experimental animal facility at Universidade Federal de São Paulo (UNIFESP). The study was approved by the Ethics Committee of UNIFESP (process number CEP 0987/11).

After the three-month treatment, mice were sacrificed by CO_2 asphyxiation and the organs/tissues collected were immediately frozen by dipping into liquid nitrogen. After being preserved with Tissue-Tek O.C.T. compound (Sakura Finetek, Torrance, CA, USA), the organs/tissues were stored in $-80\,°C$ until 4 μm-thick cryosections could be cut and mounted on slides. The following parts were collected: part of the stomach wall, part of the liver, part of the pancreas, the entire spleen, the entire right kidney, part of the heart for cardiac muscle, part of the skeletal muscle from the right back leg, part of the frontal cortex of the brain, and part of the skin from the belly.

Prior to indirect immunofluorescent staining, cryosections were removed from $-80\,°C$ and incubated with 4% paraformaldehyde in PBS for 20 min, followed by blocking with 1% bovine serum albumin for 1 h at room temperature (RT). Sections were then incubated for 1 h at RT with rabbit polyclonal anti-IMPDH2 antibody (12948-1-AP, Proteintech, Chicago, IL, USA) alone or together with a human serum It2006 with anti-RR/IMPDH reactivity previously characterized (Carcamo et al., 2011), both diluted 1:500 in PBS. After washing three times with PBS for 5 min, slides were incubated with Alexa Fluor 568-conjugated goat anti-rabbit IgG (A-11036, Thermo Fisher, Waltham, MA, USA) and DyLight 488-conjugated goat anti-human IgG (072-03-10-06, Kirkegaard & Perry Laboratories, Gaithersburg, MD, USA), both diluted 1:500 in PBS, for 40 min at RT in a dark wet chamber. After washing as before, the slides were sealed with Vectashield mounting medium with DAPI (Vector Laboratories, Burlingame, CA, USA) and analyzed under 200X, 400X, or $1000\times$ magnification with a Zeiss Axio Imager M2 fluorescence microscope (Carl Zeiss Microscopy, Jena, Germany).

For the quantification of cells that present RR structures, at least three images were captured for each tissue from each animal. The amount of cells quantified in each tissue is presented in Supplementary Table 1. The average percentage of RR-positive cells (across all 3 animals in each group) for each tissue is presented with the standard error of mean (SEM).

Author contributions

G.D.K. conceived the study, designed and performed the experiments, analyzed and interpreted data, and wrote the original draft of the manuscript; S.J.C. interpreted data and wrote the original draft of the manuscript; E.K.L.C. critically reviewed and edited the manuscript; L.E.C.A. conceived the study, designed the experiments, and critically reviewed and edited the manuscript. All authors read and approved the final manuscript.

Funding

Declarations of interest

L.E.C.A. and G.D.K. are the inventors of a pending patent (Brazil INPI deposit number #BR1020160097541) that proposes the detection of RR structures in patient cells to track adequate ingestion of RR-inducing drugs: "*Método de detecção de ingestão adequada de medicação inibidora da enzima Inosina Monofosfato Dehidrogenase I e II, uso do método e Kit para executar o método*".

Acknowledgements

Appendix A. Supplementary data

Supplementary data related to this article can be found at https://doi.org/10.1016/j.antiviral.2018.12.017.

References

Babusis, D., Curry, M.P., Kirby, B., Park, Y., Murakami, E., Wang, T., Mathias, A., Afdhal, N., McHutchison, J.G., Ray, A.S., 2018. Sofosbuvir and Ribavirin Liver Pharmacokinetics in Patients Infected with Hepatitis C Virus. Antimicrobial agents and chemotherapy, pp. 62.

Bussereau, F., Picard, M., Blancou, J., Sureau, P., 1988. Treatment of rabies in mice and foxes with antiviral compounds. Acta Virol. 32, 33–49.

Calise, S.J., Bizzaro, N., Nguyen, T., Bassetti, D., Porcelli, B., Almi, P., Barberio, G., Pesce, G., Satoh, M., Chan, E.K., 2016a. Anti-rods/rings autoantibody seropositivity does not affect response to telaprevir treatment for chronic hepatitis C infection. Auto Immun. Highlights 7, 15.

Calise, S.J., Carcamo, W.C., Ceribelli, A., Dominguez, Y., Satoh, M., Chan, E.K.L., 2014. Antibodies to rods and rings. In: Meroni, P.L., Gershwin, M.E. (Eds.), Autoantibodies, third ed. Elsevier, San Diego, pp. 161–168.

Calise, S.J., Keppeke, G.D., Andrade, L.E.C., Chan, E.K.L., 2015. Anti-rods/rings: a human model of drug-induced autoantibody generation. Front. Immunol. 6, 41.

Calise, S.J., Purich, D.L., Nguyen, T., Saleem, D.A., Krueger, C., Yin, J.D., Chan, E.K., 2016b. 'Rod and ring' formation from IMP dehydrogenase is regulated through the one-carbon metabolic pathway. J. Cell Sci. 129, 3042–3052.

Calise, S.J., Zheng, B., Hasegawa, T., Satoh, M., Isailovic, N., Ceribelli, A., Andrade, L.E.C., Boylan, K., Cavazzana, I., Fritzler, M.J., de la Torre, I.G., Hiepe, F., Kohl, K., Selmi, C., Shoenfeld, Y., Tincani, A., Chan, E.K.L., Committee, I.A.S., 2018. Reference standards for the detection of anti-mitochondrial and anti-rods/rings autoantibodies. Clin. Chem. Lab. Med. 56, 1789–1798.

Carcamo, W.C., Calise, S.J., von Muehlen, C.A., Satoh, M., Chan, E.K.L., 2014. Molecular cell biology and immunobiology of mammalian rod/ring structures. Int. Rev. Cell Molecular Biol. 308, 35–74.

Carcamo, W.C., Satoh, M., Kasahara, H., Terada, N., Hamazaki, T., Chan, J.Y., Yao, B., Tamayo, S., Covini, G., von Muhlen, C.A., Chan, E.K., 2011. Induction of cytoplasmic rods and rings structures by inhibition of the CTP and GTP synthetic pathway in mammalian cells. PLoS One 6, e29690.

Carrier, P., Essig, M., Debette-Gratien, M., Sautereau, D., Rousseau, A., Marquet, P., Jacques, J., Loustaud-Ratti, V., 2016. Anti-hepatitis C virus drugs and kidney. World J. Hepatol. 8, 1343–1353.

Chang, C.C., Keppeke, G.D., Sung, L.Y., Liu, J.L., 2018. Interfilament interaction between IMPDH and CTPS cytoophidia. FEBS J. 285, 3753–3768.

Chang, C.C., Lin, W.C., Pai, L.M., Lee, H.S., Wu, S.C., Ding, S.T., Liu, J.L., Sung, L.Y., 2015. Cytoophidium assembly reflects upregulation of IMPDH activity. J. Cell Sci. 128, 3550–3555.

Climent, J., Morandeira, F., Castellote, J., Xiol, J., Niubo, J., Calatayud, L., Mestre, M., Bas, J., 2016. Clinical correlates of the "rods and rings" antinuclear antibody pattern. Autoimmunity 49, 102–108.

Colombo, G., Lorenzini, L., Zironi, E., Galligioni, V., Sonvico, F., Balducci, A.G., Pagliuca, G., Giuliani, A., Calza, L., Scagliarini, A., 2011. Brain distribution of ribavirin after intranasal administration. Antivir. Res. 92, 408–414.

Covini, G., Carcamo, W.C., Bredi, E., von Muhlen, C.A., Colombo, M., Chan, E.K., 2012. Cytoplasmic rods and rings autoantibodies developed during pegylated interferon and ribavirin therapy in patients with chronic hepatitis C. Antivir. Ther. 17, 805–811.

Endres, C.J., Moss, A.M., Ke, B., Govindarajan, R., Choi, D.S., Messing, R.O., Unadkat, J.D., 2009. The role of the equilibrative nucleoside transporter 1 (ENT1) in transport and metabolism of ribavirin by human and wild-type or Ent1-/- mouse erythrocytes. J. Pharmacol. Exp. Therapeut. 329, 387–398.

Galli, A., Mens, H., Gottwein, J.M., Gerstoft, J., Bukh, J., 2018. Antiviral effect of ribavirin against HCV associated with increased frequency of G-to-A and C-to-U transitions in infectious cell culture model. Sci. Rep. 8, 4619.

Gish, R.G., 2006. Treating HCV with ribavirin analogues and ribavirin-like molecules. J. Antimicrob. Chemother. 57, 8–13.

Gunter, J.H., Thomas, E.C., Lengefeld, N., Kruger, S.J., Worton, L., Gardiner, E.M., Jones, A., Barnett, N.L., Whitehead, J.P., 2008. Characterisation of inosine monophosphate dehydrogenase expression during retinal development: differences between variants and isoforms. Int. J. Biochem. Cell Biol. 40, 1716–1728.

Jeulin, H., Venard, V., Carapito, D., Finance, C., Kedzierewicz, F., 2009. Effective

ribavirin concentration in mice brain using cyclodextrin as a drug Carrier: evaluation in a measles encephalitis model. Antivir. Res. 81, 261–266.

Ji, Y., Gu, J., Makhov, A.M., Griffith, J.D., Mitchell, B.S., 2006. Regulation of the interaction of inosine monophosphate dehydrogenase with mycophenolic acid by GTP. J. Biol. Chem. 281, 206–212.

Keppeke, G.D., Andrade, L.E., Grieshaber, S.S., Chan, E.K., 2015. Microinjection of specific anti-IMPDH2 antibodies induces disassembly of cytoplasmic rods/rings that are primarily stationary and stable structures. Cell Biosci. 5, 1.

Keppeke, G.D., Calise, S.J., Chan, E.K., Andrade, L.E., 2016a. Anti-rods/rings autoantibody generation in hepatitis C patients during interferon-alpha/ribavirin therapy. World J. Gastroenterol. 22, 1966–1974.

Keppeke, G.D., Chang, C.C., Peng, M., Chen, L.Y., Lin, W.C., Pai, L.M., Andrade, L.E.C., Sung, L.Y., Liu, J.L., 2018. IMP/GTP balance modulates cytoophidium assembly and IMPDH activity. Cell Div. 13, 5.

Keppeke, G.D., Nunes, E., Ferraz, M.L., Silva, E.A., Granato, C., Chan, E.K., Andrade, L.E., 2012. Longitudinal study of a human drug-induced model of autoantibody to cytoplasmic rods/rings following HCV therapy with ribavirin and interferon-alpha. PLoS One 7, e45392.

Keppeke, G.D., Prado, M.S., Nunes, E., Perazzio, S.F., Rodrigues, S.H., Ferraz, M.L., Chan, E.K., Andrade, L.E., 2016b. Differential capacity of therapeutic drugs to induce Rods/Rings structures in vitro and in vivo and generation of anti-Rods/Rings autoantibodies. Clin. Immunol. (Orlando, Fla.) 173, 149–156.

Markland, W., McQuaid, T.J., Jain, J., Kwong, A.D., 2000. Broad-spectrum antiviral activity of the IMP dehydrogenase inhibitor VX-497: a comparison with ribavirin and demonstration of antiviral additivity with alpha interferon. Antimicrob. Agents Chemother. 44, 859–866.

Novembrino, C., Aghemo, A., Ferraris Fusarini, C., Maiavacca, R., Matinato, C., Lunghi, G., Torresani, E., Ronchi, M., Garlaschi, M.C., Ramondetta, M., Colombo, M., 2014. Interferon-ribavirin therapy induces serum antibodies determining 'rods and rings' pattern in hepatitis C patients. J. Viral Hepat. 21, 944–949.

Paeshuyse, J., Dallmeier, K., Neyts, J., 2011. Ribavirin for the treatment of chronic hepatitis C virus infection: a review of the proposed mechanisms of action. Curr. Opinion Virol. 1, 590–598.

Probst, C., Radzimski, C., Blocker, I.M., Teegen, B., Bogdanos, D.P., Stocker, W., Komorowski, L., 2013. Development of a recombinant cell-based indirect immunofluorescence assay (RC-IFA) for the determination of autoantibodies against "rings and rods"-associated inosine-5′-monophosphate dehydrogenase 2 in viral hepatitis C. Clin. Chim. Acta Int. J. Clin. Chem. 418, 91–96.

Seelig, H.P., Appelhans, H., Bauer, O., Bluthner, M., Hartung, K., Schranz, P., Schultze, D., Seelig, C.A., Volkmann, M., 2011. Autoantibodies against inosine-5'-monophosphate dehydrogenase 2–characteristics and prevalence in patients with HCV-infection. Clin. Lab. 57, 753–765.

Sidwell, R.W., Allen, L.B., Khare, G.P., Huffman, J.H., Witkowski, J.T., Simon, L.N., Robins, R.K., 1973. Effect of 1-beta-D-ribofuranosyl1-1,2,4-triazole-3-carboxamide (virazole, ICN 1229) on herpes and vaccinia keratitis and encephalitis in laboratory animals. Antimicrob. Agents Chemother. 3, 242–246.

Stinton, L.M., Myers, R.P., Coffin, C.S., Fritzler, M.J., 2013. Clinical associations and potential novel antigenic targets of autoantibodies directed against rods and rings in chronic hepatitis C infection. BMC Gastroenterol. 13, 50.

Testoni, B., Levrero, M., Durantel, D., 2014. Mechanism of action of ribavirin in anti-HCV regimens: new insights for an age-old question? Gut 63, 3–4.

Welsch, C., Jesudian, A., Zeuzem, S., Jacobson, I., 2012. New direct-acting antiviral agents for the treatment of hepatitis C virus infection and perspectives. Gut 61 (Suppl. 1), i36–46.